ParCFD2022
33^{rd} International Conference on Parallel Computational Fluid Dynamics
May 25-17 2022, Alba Italy

TRANSPIRATION COOLING OF HYPERSONIC FLOW PAST A FLAT PLATE WITH POROUS INJECTION

Pushpender K. Sharma*, Ralf Deiterding* AND Neil Sandham*

* University of Southampton
Aeronautics and Astronautics Department
Boldrewood Innovation Campus, Burgess Rd, Southampton SO16 7QF, United Kingdom
e-mail: p.k.sharma@soton.ac.uk, r.deiterding@soton.ac.uk, n.sandham@soton.ac.uk, web page: https://www.southampton.ac.uk/

Key words: Hypersonic flows, transition, Transpiration cooling, porous layer

Abstract. Transpiration-based cooling using porous layer is explored where the coolant is injected into the hypersonic cross-flow, providing a more uniform distribution of the coolant. Three-dimensional direct numerical simulations of flow past a flat plate with a porous layer are conducted at $M = 5$. Conjugate heat flux boundary condition is used as compared to the simpler isothermal wall. The coolant is injected through a porous layer composed of a staggered (body-centered cubic) arrangement of spheres. Smaller pressure ratios resulting in relatively smaller blowing ratios are used, which are found to be more effective in the experiments. Also, to mimic turbulent conditions in the experiments, wall-bounded disturbances are introduced upstream of the porous layer such that reasonable mixing of coolant is allowed inside the hypersonic boundary layer. It is noted from the moderately high Reynolds number cases that the lowest blowing ratio results in more cooling immediately downstream of the porous layer, while the highest blowing ratio show higher effectiveness farther downstream.

1 INTRODUCTION

Various coolant injection techniques [1, 2] have been explored in the past to reduce the heat loads on the surface of high-speed vehicles. Two main techniques used are, namely, a) effusion cooling [1], where the injection occurs through localised holes, b) transpiration cooling [2, 3], in which coolant transpires more uniformly through the surface of a porous material. The transpiration cooling methods are regarded more efficient due to the enhanced heat exchange between coolant and structure with multiple pores of micrometer dimension [2], while effusion through holes/slots might cause early transition, hence reducing the laminar stretch of the boundary layer. This suggests a need to further explore the benefits of using transpiration-based cooling systems. Direct numerical simulations (DNS) are a very useful tool to do such studies with capability to capture details.

2 THE SOLVER AND THE NUMERICAL SET-UP

The solver used is an in-house solver, called AMROC (Adaptive Mesh Refinement using Object Oriented Cpp) [4]. It is a finite-volume-based solver with structured adaptive mesh

refinement capability which allows for higher resolution in the small pore length scales of the porous layer. The system of 3D dimensionless governing equations for compressible Navier-Stokes equations are solved in conservation form, under the assumption of constant specific heats, along with the species conservation equation to trace the concentration of the coolant in the flow [4]. A hybrid WENO-CD scheme is used, i.e., 6^{th}-order central differencing (CD) scheme in space for both inviscid and viscous fluxes, combined with a 6^{th}-order weighted-essentially-non-oscillatory (WENO) scheme for shock capturing. A 3^{rd}-order Runge-Kutta method is used for time integration.

The numerical set-up is inspired by the experiments performed at Oxford Thermofluids Institute using the ultra high temperature ceramic (UHTC) as the porous material [3]. The free-stream condition are M=5, T^*_∞=76.66 K, ρ^*_∞=0.07979 Kg/m^3 and p^*_∞=1.75$\times$10^3 Pa, which results in a unit Reynolds number of $Re/m = 12.6 \times 10^6$. The computation domain is a 3D rectangular box with periodicity in the spanwise (z) direction. The extents of the domain in x-, y-, and z-directions are 0 to 160, -1.28 to 22.72, and -4 to 4, respectively. The inflow plane of the computational domain (at x=0) is located approximately at $\tilde{x}^*$=127 mm from the leading edge of the flat plate such that the displacement thickness at inflow plane is δ^*=1 mm, which is also used as the characteristic length scale and hence Re_{δ^*}=12600 is used in the simulations. A grid with $N_x \times N_y \times N_z = 2000 \times 300 \times 100$ cells is used for the coarsest level. Two levels of refinement are used to ensure enough resolution in the porous layer region. It takes about 48000 cpu-hours to reach $t \approx 500$ using 400 processor cores. The flat plate is placed at $y = 0$ and has a porous layer section of length and width 39 mm $\times$ 8 mm placed between $x = 35$ and $x = 74$. The starting location of the porous layer determines the Reynolds number at the injection location, i.e., at $x = 35$ or $\tilde{x} = 127 + 35$, $R_{inj} = 2.04 \times 10^6$.

The artificial porous layer is created with a staggered arrangement of spheres (body-centered cubic, BCC) to blow the coolant uniformly into the oncoming hypersonic cross-flow. Various pressure ratios (PR) are chosen such that similar blowing ratios (BR) as observed in the experiments are obtained numerically, maintaining similar coolant mass efflux; see Table 1. The blowing-suction disturbances of the form, $v'(x, z, t) = A\cos(\beta_0 z)\cos[\alpha_0(x - x_0) - \omega_0 t]$, are imposed in the v-component of velocity at $y = 0$ between $x = 10$ to 30. More realistic conjugate heat flux (CHF) boundary conditions are used at the wall compared to simpler isothermal wall, where heat fluxes from the fluid and solid side are equated to obtain the surface temperature.

3 RESULTS

Table 1 presents the list of 3D numerical simulations performed. A representative 3D picture of the flow field is shown in Fig. 1 for Case-2, where coolant concentration, Schileren, and u-component of velocity are presented on x-z, y-z, and x-y planes, respectively. The coolant concentration is shown at $y = 0.5$, showing higher concentration above the porous layer while it decreases as one moves downstream. As the boundary layer, shown through u-velocity component on the side plane, transitions to turbulence around $x \approx 100$, the coolant also starts to get mixed within the boundary layer. A quan-

Table 1: Cases considered for $Re_{inj} = 2.04 \times 10^6$

Case No.	PR	BR	Disturbance Amplitude
1	1	0	5%
2	1.15	0.0020	5%
3	1.3	0.0030	5%
4	1.5	0.0065	5%

titative picture of the flow field is shown in Fig. 2, comparing span-time averaged heat fluxes among various cases. It can be noted from Fig. 2 that the lowest PR/BR case, Case-2, shows the lowest heat flux values downstream of the porous layer till $x \approx 105$, while intermediate PR/BR case, Case-3, shows the highest value in the vicinity of the porous layer. This can also be noted from the corresponding plots in the bottom figure for effectiveness, $\eta = (1 - q_{w,c}/q_{w,nc})$, where $q_{w,c}$ and $q_{w,nc}$ are the wall heat fluxes with and without coolant, respectively. However, highest PR/BR case, Case-4, gives the best cooling effectiveness over a longer stretch of flat plate downstream of the porous layer. This happens as for the highest PR/BR case, the transition occurs earlier over the porous layer itself, causing higher coolant mixing while having the highest amount of coolant concentration among all cases. However, for the intermediate PR/BR case, though the transition occurs earlier the coolant concentration is significantly less. For the lowest PR/BR case, coolant forms a film immediately downstream of porous layer which creates highest cooling and only stars to transition at a downstream location beyond $x \approx 105$, worsening the performance.

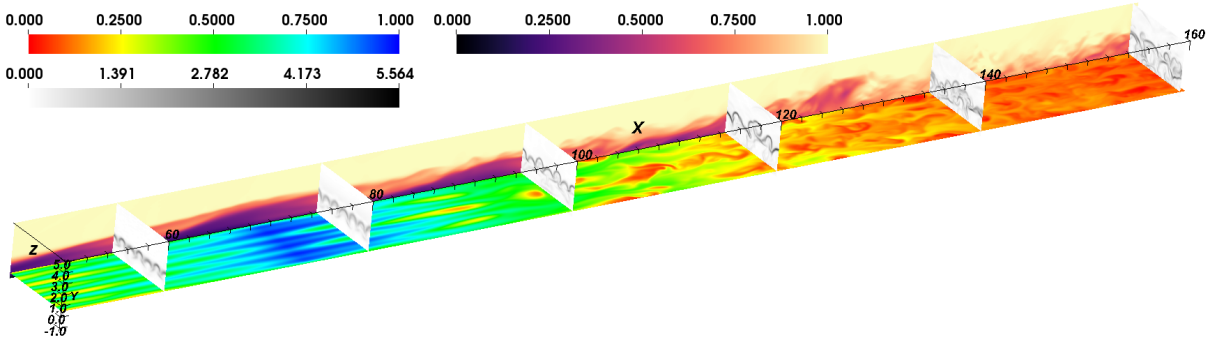

Figure 1: 3D view of flow field for Case-2, showing a) coolant concentration on x-z plane at $y = 0.5$, b) Schlieren on various y-z planes along x-direction, c) u-velocity component on x-y plane at $z = -4$.

4 CONCLUSIONS

Higher heat flux values are noted for the intermediate PR/BR case. The lowest PR/BR case, is most effective immediately downstream of the porous layer; however, the performance degrades father downstream. The highest PR/BR case, shows the highest effectiveness over a longer stretch downstream of the porous layer. Higher Reynolds

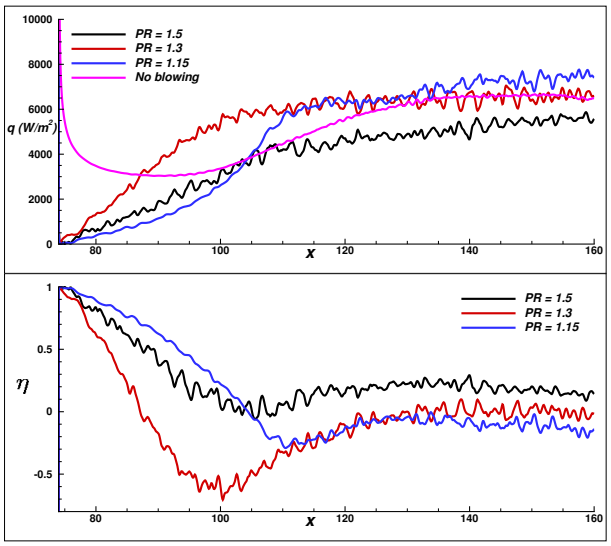

Figure 2: Heat fluxes for different cases in the top frame while cooling effectiveness in the bottom frame, starting from the trailing edge of porous layer at $x = 74$.

number ($Re_{inj} = 2.18 \times 10^6$) cases (not presented here) are also simulated. For these case, the wall heat-flux values continuously decrease, and cooling efficiencies also continuously increase with increasing PR/BR. So from the various cases for the two Reynolds numbers, in general, a relatively higher pressure/blowing ratio tends to provide higher cooling effectiveness over a larger stretch and therefore could be used in an application scenario where multiple porous layer sections are placed slightly farther apart from each other. A detailed description of the flow physics along with various comparisons will be presented.

REFERENCES

[1] M. A. Keller and M. J. Kloker, "Direct numerical simulation of foreign-gas film cooling in supersonic boundary-layer flow," *AIAA J.*, vol. 55, no. 1, pp. 99–111, 2017.

[2] T. Langener, J. V. Wolfersdorf, and J. Steelant, "Experimental investigations on transpiration cooling for scramjet applications using different coolants," *AIAA J.*, vol. 49, no. 7, pp. 1409–1419, 2011.

[3] T. Hermann, H. S. Ifti, M. McGilvray, L. Doherty, and R. P. Geraets, "Mixing characteristics in a hypersonic flow around a transpiration cooled flat plate model," in *HiSST: Int. Conf. on High-Speed Vehicle Science Technology*, (Moscow, Russia), 2018.

[4] A. Cerminara, R. Deiterding, and N. Sandham, "A mesoscopic modelling approach for direct numerical simulations of transition to turbulence in hypersonic flow with transpiration cooling," *Int. J. Heat and Fluid Flow*, vol. 86, p. 108732, 2020.